Fibers and Polymers 2020, Vol.21, No.11, 2440-2447
DOI 10.1007/s12221-020-9667-4

ISSN 1229-9197 (print version)
ISSN 1875-0052 (electronic version)

Adsorption of Bovine Serum Albumin onto Tannic Acid-Immobilized Chitosan Resin

Hai-yan Li*, Hai-mei Liu, and Qin Zhao

School of Food Engineering, Lu Dong University, Yantai 264025, China
(Received June 25, 2019; Revised February 22, 2020; Accepted February 25, 2020)

Abstract: A novel tannic acid-immobilized chitosan resin (TICR) was prepared by Mannich reaction for the adsorption of proteins. The physical properties of TICR were characterized and the effects of contact time, pH, and initial concentration of (bovine serum albumin) BSA on its adsorption by TICR were investigated. The Langmuir isotherm model was applied to describe the adsorption isotherm. The equilibrium data are fitted to the Langmuir isotherm model. The maximum monolayer BSA adsorption capacities of TICR were found to be 1.094, 1.487, and 1.694 mg/g at 298, 308, and 318 K, respectively. Furthermore, the data were analyzed on the basis of pseudo-first order, pseudo-second order, and intraparticle diffusion models. The correlation results suggested that the pseudo-second order model fitted the experimental data very well. The thermodynamic study indicated that the adsorption process of BSA onto TICR was endothermic, and the Gibbs free energy (ΔG^{o}), enthalpy (ΔH^{o}), and entropy (ΔS^{o}) of the adsorption process were calculated according adsorption isotherm data. TICR could be reused for 10 times with only 19 % loss of adsorption capacity for BSA.

Keywords: Chitosan, Tannic acid, Immobilized, BSA, Adsorption

Introduction

Chitosan is a linear polysaccharide produced by partial deacetylation of chitin. It is composed of randomly distributed β-(1,4) linked D-glucosamine and N-acetyl-D-glucosamine [1]. Chitosan has turned to be one of the most important natural polymers due to nontoxicity, biodegradability, biocompatibility, bioactivity, and attractive physical and mechanical performances [2]. Meanwhile, chitosan contains abundant amino and hydroxyl groups, making it quite potential as an excellent adsorbent for proteins, phenols, organic acids, dyes, and metal ions [3,4]. However, chitosan swells and dissolves readily in acidic solutions, which limits its application as an adsorbent in acidic media. Accordingly, its crosslinking should be taken into consideration. The existence of amino and hydroxyl groups renders the chemical modification of chitosan possible. Many methods have been reported to modify chitosan, such as reverse phase suspension cross-linking polymerization, emulsification, spray drying, grafting, oligomerization, and alkylation [3-8].

In our previous study, the chitosan resin was prepared by reverse phase suspension cross-linking polymerization and the resin was used as a protein adsorbent for beer and juice clarification [8]. The results showed that the resin can adsorb proteins, phenols, organic acids, and metal ions from beer and juice [9,10]. But the chitosan resin lacked the unique affinity for protein adsorption. Therefore, the chitosan resin can serve as promising adsorbents to adsorb proteins effectively if it is further grafted or modified by suitable functional groups. Chitosan can be modified through many methods, such as grafting, oligomerization, alkylation, and etc [11-13]. Hua *et al.* designed and carried out the affinity adsorption purification of His-tagged proteins using EDTA-chitosan-based adsorption [14]. Zeng *et al.* prepared chitosan/poly(ε-caprolactone) blend films in different mass ratios to adsorb BSA [15].

It is well-known that tannic acid (TA) contains multiple adjacent phenolic hydroxyls and exhibits specific affinity for proteins. The main advantage of TA is its ability to combine protein. Many researchers have used TA as a cross-linking agent for chitosan. Rivero *et al.* modified chitosan films by TA as a cross-linking agent [16]. Beata Kaczmarek *et al.* treated collagen and chitosan mixtures with TA [17]. In addition, it has been reported that TA can be immobilized onto activated carbon, collagen fiber, agarose, and other matrices [18-24]. However, in the literature there is no information about the modification of chitosan resin with TA.

Furthermore, TA can react with an amino compound through Mannich reaction [18]. So it is feasible that TA could be immobilized onto chitosan. It can be inferred that TA immobilized onto chitosan resin should significantly increase the adsorption capacity for protein. Therefore, we have a hypothesis that chitosan resin could be modified by TA to improve the protein uptake capacity.

The aim of this study was to prepare the TA modified chitosan resin as the promising adsorbents for efficient removal of proteins from aqueous solutions for food industry, such as beer, juice, and aquatic processing wastewater. BSA was selected as a model to investigate the effect of the modification on the protein adsorption behavior of chitosan resin. The desorption efficiency and the reusability of the resins were finally evaluated.

*Corresponding author: haiyanli19814@163.com

Experimental

Materials

Chitosan with deacetylation degree of 90 % (M_η=5.5×10^5) was purchased from Qingdao Biochemical Co. (Qingdao, China). BSA was purchased from Sigma (St. Louis, MO, USA). Glutaraldehyde, formaldehyde, liquid paraffin, Span 80, TA, NaOH, HCl, acetone, and ethanol were of analytical grade and were purchased from Sinopharm Chemical reagent Co., Ltd. (Shanghai, China).

Preparation of Chitosan Resin (CR)

A total of 5 g of chitosan powder was suspended in 100 m*l* of 2 % (v/v) acetic acid solution and left overnight for complete dissolution. Then, the dispersant agent liquid paraffin (100 m*l*) was added to the chitosan solution and mixed well with stirring followed by the addition of 5 m*l* Span 80 as an emulsifier. Then, 20 m*l* of 37 % (w/w) formaldehyde solution was added to the emulsion drop by drop for cross-linking. Half an hour later, the pH value was adjusted to 10 by 2 mol/*l* NaOH solution and 10 m*l* epichlorohydrin was added for further cross-linking for another 2 h. The suspension was finally filtered and the solid was collected and soaked in 0.1 mol/*l* HCl with stirring for 1 h at room temperature to remove formaldehyde. The supernatant was discarded and the resins were further washed with acetone, ethanol, and distilled water in sequence for 3 times. The chitosan resin (CR) was collected and vacuum dried for subsequent experiments.

Preparation of TA-Immobilized Chitosan Resin (TICR)

TICR was prepared by immobilizing TA onto chitosan by Mannich reaction. The preparation procedure is illustrated in Figure 1.

A total of 1 g CR was immersed in 20 m*l* water at room temperature for 2 h. Then, 2 m*l* 37 % (w/w) formaldehyde solution was added and the mixture was stirred at 40 °C for 30 min. After the incubation completed, 20 m*l* 1 % (w/w) TA solution was added and the pH value was adjusted to 10 by 2 mol/*l* NaOH solution. Subsequently, the temperature was rapidly increased to 60 °C to allow the Mannich reaction under nitrogen atmosphere. Five hours later, the mixture was filtered and the resin was washed with distilled water and vacuum-dried at 60 °C for 12 h. The resultant

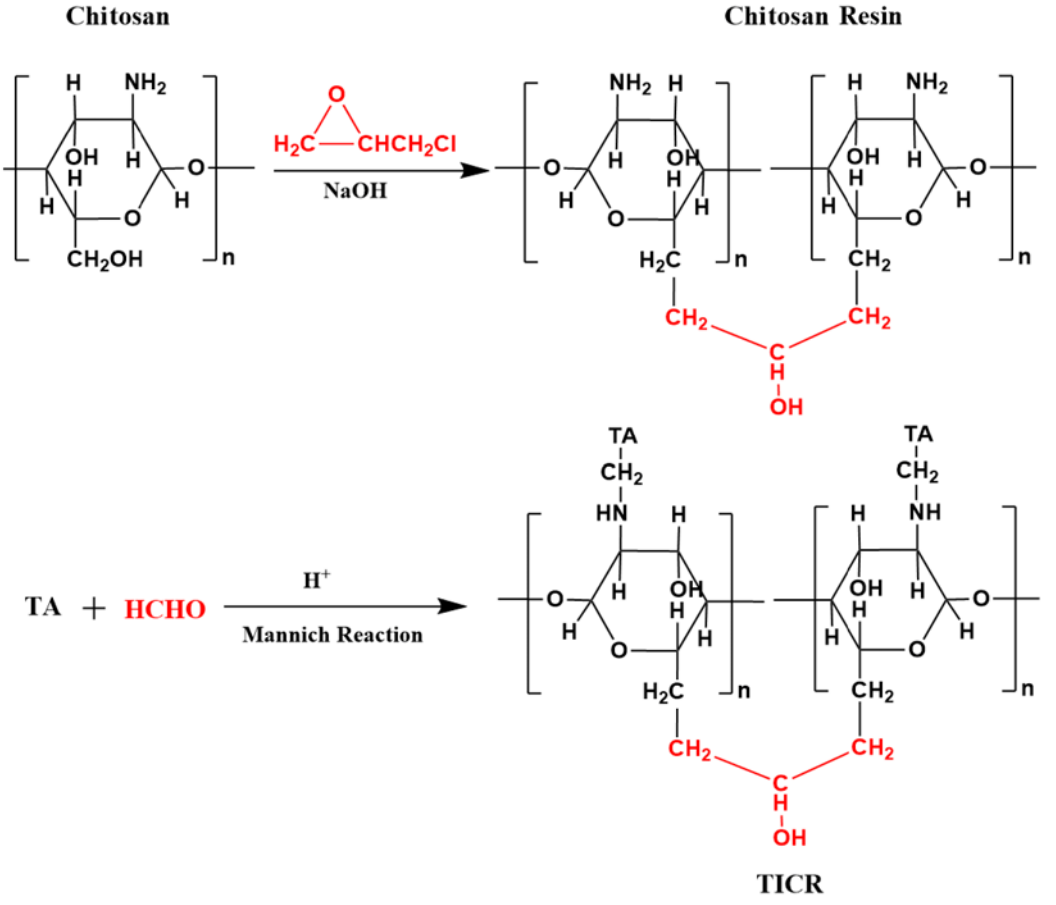

Figure 1. Schematic diagram for the preparation mechanism of TICR through the Mannich reaction.

resin was collected and designated as TICR.

Characterization of TICR

The water content (H), skeletal density (ρ_T), pileup density (ρ_p), and porosity degree (P) of TICR were characterized according to the methods mentioned in a previous report [8].

The morphology of TICR was observed by using a scanning electron microscope (SEM) (JSM-6390LV, JEOL Ltd., Japan). Samples were coated by fine gold palladium film before SEM observation. The particle size distribution (PSD) of TICR was studied by a Malvern Mastersizer 2000 (Malvern, U K).

Adsorption Behavior

The protein adsorption behavior of TICR obtained was studied by using BSA as a model. All the adsorption experiments were carried out by using batch adsorption technique (0.1 g TICR or CR in 20 m*l* BSA solution). The adsorption of TICR or CR to BSA was investigated by contact time, initial BSA concentrations (20 to 70 mg/*l*), and various pH values (pH was selected at 4.0, 5.0, 6.0, 7.0, and 8.0) in 0.1 mol/*l* phosphate buffer solution. The adsorption process was allowed to occur at 298 K with 120 rpm stirring for 300 min. The concentration of BSA in the filtrate was analyzed by Bradford method. The adsorption capacity at time t (min) was calculated according to the mass change of BSA before and after adsorption and was denoted as q_t (mg/g).

Adsorption Kinetics

An exact amount of 0.1 g TICR was suspended in 20 m*l* of 50 mg/*l* BSA solution (in 0.1 mol/*l* pH 6.0 phosphate buffer). The adsorption process was conducted at 298, 308, and 318 K with constant stirring for 300 min. The suspension was filtered and the concentration of BSA in filtrate was analyzed by Bradford method at a regular interval during adsorption process.

Adsorption Isotherms

An exact amount of 0.1 g TICR was soaked in 20 m*l* BSA solutions of a series concentration ranging from 20 to 70 mg/*l* and maintained at 298, 308, and 318 K for 300 min. The changes of BSA concentration in the solution after the adsorption were measured by the Bradford method. The equilibrium adsorption capacity of the resins was then calculated according to the following formula as equation (1) [25]:

$$q_e = \frac{(C_0 - C_e)V}{W} \quad (1)$$

where q_e is the equilibrium adsorption capacity of TICR (mg/g), C_0 and C_e are the initial and equilibrium solution concentrations (mg/*l*) of BSA, respectively. V is the volume of the solution (m*l*), and W is the weight of TICR used (g).

All the experiments were repeated in triplicate and the average values were presented.

Desorption and Reusability Evaluation

Desorption studies are very important since the economic success of the adsorption process depends on the reusability of the developed adsorbent [26]. In this work, 0.1 mol/*l* HCl aqueous solutions were used to regenerate TICR, and the procedure was repeated for many times until BSA could no longer be detected in the filtrate. Then TICR was washed thoroughly with double-distilled water until the filtrate became neutral and subjected to reusability evaluation in the following conditions: TICR/BSA solution radio (m/v)= 1:200, contact time 150 min, temperature 298 K, solution pH 6.0, and BSA concentration solution 50 mg/*l*. The procedure was repeated 10 times.

Results and Discussion

Characterization of TICR

The properties of TICR are displayed in Table 1 and Figure 2. The water content (H) and porosity degree (P) of the resin were 61.230 % and 0.733, respectively. The porous structure could provide abundant sites for protein adsorption. PSD analysis (Figure 3) reveals only one peak and 90 % of the TICR particles fell in the range of 275-500 μm indicating the narrow size distribution of the resins and the average particle size of about 417 μm.

Effects of Contact Time on BSA Adsorption

Figure 4 shows the variations of adsorption capacities (q_t) of BSA onto TICR and CR as a function of contact time. It could be seen that q_t increased with the elongation of contact

Table 1. Physical properties of TICR

Water content H (%)	Pileup density ρ_P (g/m*l*)	Skeletal density ρ_T (g/cm^3)	Porosity degree P
61.230±1.056	0.902±0.074	1.739±0.120	0.733±0.035

Values were given as average±standard deviation.

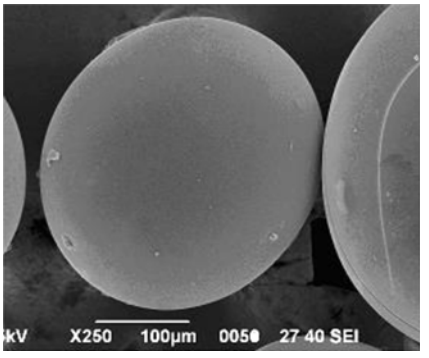

Figure 2. SEM micrograph of TICR.

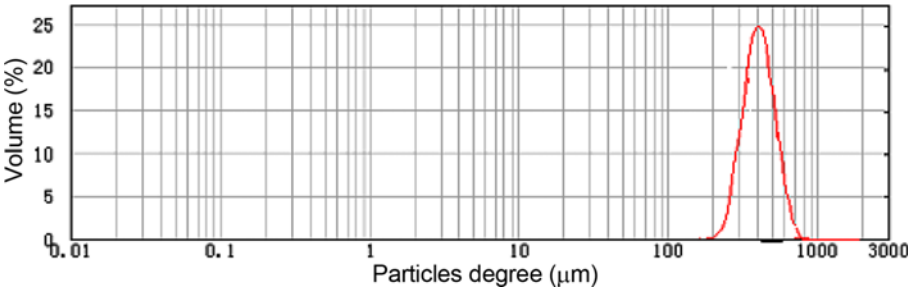

Figure 3. Particle size distribution of TICR.

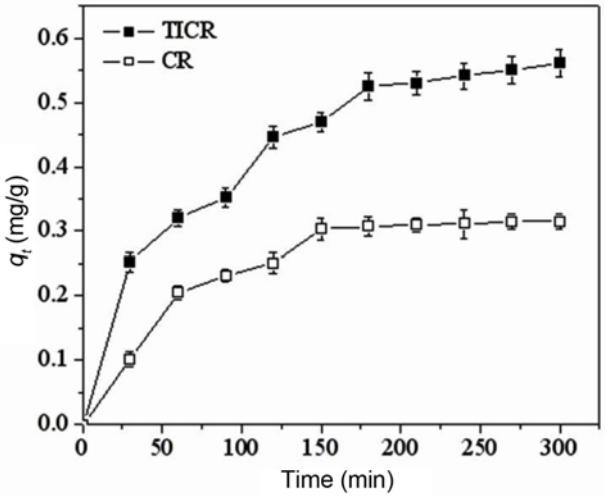

Figure 4. Effect of contact time on BSA adsorption capacities of TICR and CR (C_0: 30 mg/*l*, temperature: 298 K, pH: 7.0).

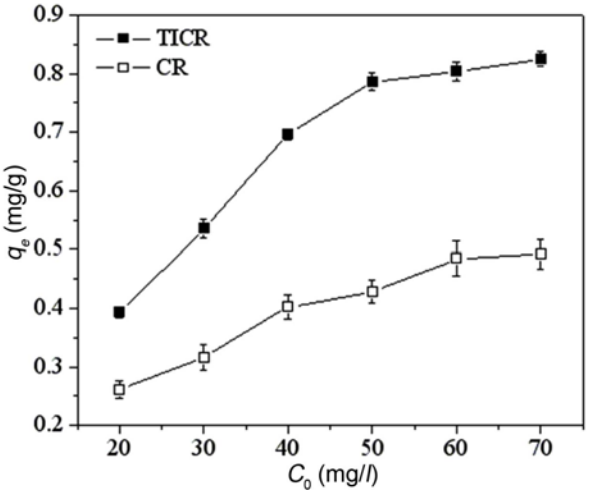

Figure 5. Effect of initial BSA concentration on its adsorption by TICR and CR (time: 300 min, temperature: 298 K, pH: 7.0).

time and the absorption occurs fastest within 180 min, which increased sharply to 0.525 mg/g and 0.307 mg/g, respectively, for TICR and CR. As the contact time further increases to 300 min, q_t increased slowly only by 0.036 mg/g and 0.008 mg/g, indicating that adsorption equilibrium had been reached. Therefore, 300 min can be considered as the equilibrium time required for maximum adsorption of BSA and equilibrium BSA adsorption capacities of TICR and CR were 0.561 mg/g and 0.315 mg/g, respectively. This result indicates that the introduction of TA can markedly improve the adsorption ability of CR.

Effect of Initial BSA Concentrations on Its Adsorption

Figure 5 shows plots of the equilibrium adsorption capacities (q_e) of BSA onto TICR and CR versus initial BSA concentrations at 298 K. The equilibrium adsorption capacity increased greatly as the initial BSA concentration grew from 20 mg/*l* to 50 mg/*l*. The equilibrium adsorption capacities of CR and TICR for BSA were as low as 0.261 and 0.393 mg/g in initial BSA concentration 20 mg/*l*; as the initial BSA concentration increased to 50 mg/*l*, the adsorption capacities raised markedly to 0.428 and 0.786 mg/g. The increase in q_e of TICR was more significant than that of CR. When the initial BSA concentration further increased from 50 mg/*l* to 70 mg/*l*, the equilibrium adsorption capacity increased slowly. The results suggested that the initial concentration played an important role in the adsorption capacity of BSA on TICR.

The increase of equilibrium BSA adsorption capacity (q_e) with initial BSA concentration rise might be attributed to the enhanced driving force caused by concentration gradient. After the reactive sites for BSA adsorption of the resins are saturated, further increase of the initial BSA concentration could not lead to more absorption [27,28].

Effect of pH on BSA Adsorption

The effect of pH on the adsorption capacity of BSA was investigated (Figure 6). The optimal pH of TICR for BSA adsorption mainly depends on the nature of TICR and the three-dimensional structure of BSA [29]. The isoelectric point of BSA is 4.9 [30]. When the solution pH is lower than 4.9, both BSA and TICR carry positive charges and the electrostatic repulsion between BSA and TICR. In the pH range 4.9-6.0, BSA is negatively charged, but TICR is still

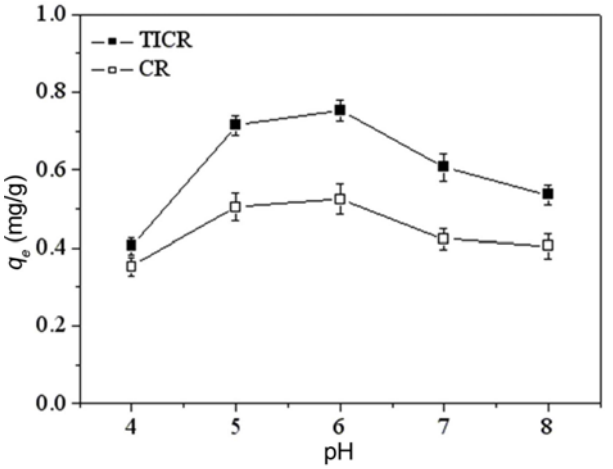

Figure 6. Effect of pH on the BSA adsorption of TICR and CR (time: 300 min, temperature: 298 K, C_0: 50 mg/*l*).

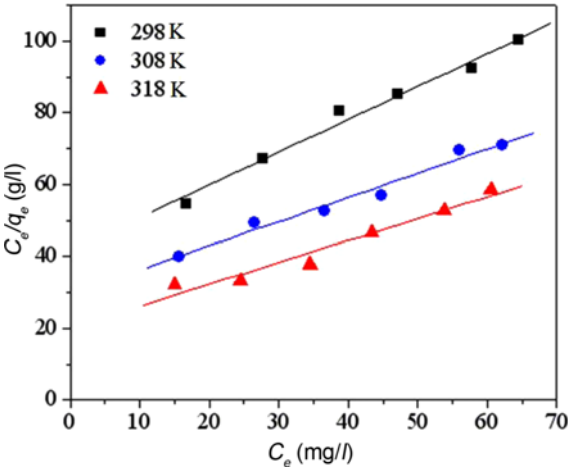

Figure 7. Langmuir plots for the adsorption of BSA onto TICR at various temperatures.

with positively charged and hence strong electrostatic attraction occurs between them. Figure 6 revealed that the maximum BSA adsorption occurred at pH 6.0. As the solution pH increased to 7.0-8.0, both BSA and TICR carry negative charges and electrostatic repulsion hinders their binding, leading to decreased q_e.

BSA Adsorption Isotherms of TICR

The analysis of equilibrium data is important for evaluating the adsorption properties of an adsorbent. The isotherm equation, namely Langmuir isotherm model, has been used for the study of adsorption behavior. The Langmuir isotherm model assumes that adsorption takes place at uniform energy sites on the surface of the adsorbent.

The Langmuir isotherm equation can be expressed as equation (2) [31]:

$$\frac{C_e}{q_e} = \frac{1}{K_b q_s} + \frac{C_e}{q_s} \tag{2}$$

where q_s (mg/g) is the saturation adsorption capacity of the monolayer, while q_e (mg/g) and C_e (mg/*l*) represent adsorption capacity and concentration in the solution at equilibrium, respectively, and K_b is the Langmuir binding constant which is related to the energy of adsorption (*l*/mg).

Additionally, the degree of suitability of TICR towards BSA adsorption was estimated from the values of the separation factor constant (R_L). R_L was calculated to identify whether an adsorption system is favorable or unfavorable [32]. The separation factor R_L is defined as equation (3):

$$R_L = \frac{1}{1 + K_b C_0} \tag{3}$$

where K_b is the Langmuir equilibrium constant (*l*/mg) and C_0 is the initial concentration of BSA (mg/*l*). When the R_L value was greater than 1, between 0 and 1, 0, or 1, the adsorption was regarded unfavorable, favorable, irreversible, or linear, respectively [33,34].

The adsorption data fitted with the Langmuir isotherm model is shown in Figure 7 and Table 2. The R^2 values for the Langmuir isotherm models were all above 0.90, suggesting that the Langmuir model fits the experimental results very well. The values of R_L were all in the range of $0<R_L<1$, indicating that the adsorption of BSA on TICR was favorable. Thus, TICR is the favorable adsorbent. In addition, the values of q_s increased evidently with the rise of temperature.

Adsorption Kinetics of TICR for BSA

In order to elucidate the adsorption kinetic mechanism, pseudo-first order equation, pseudo-second order, and intra-particle diffusion models were employed to interpret the experimental data [35,36]. A good correlation of the kinetic data explains the adsorption mechanism of BSA on TICR. The best-fit model was selected according to the linear regression correlation coefficient values (R^2).

The linear pseudo-first-order equation can be described as

Table 2. Langmuir isotherm parameters for BSA with TICR

T (K)	Langmuir isotherm equation	q_s (mg/g)	K_b (*l*/mg)	R^2	R_L
298	C_e/q_e=41.6+0.9139C_e	1.094	0.022	0.9854	0.695
308	C_e/q_e=29.515+0.6723C_e	1.487	0.023	0.9728	0.687
318	C_e/q_e=20.176+0.6066C_e	1.649	0.030	0.9573	0.624

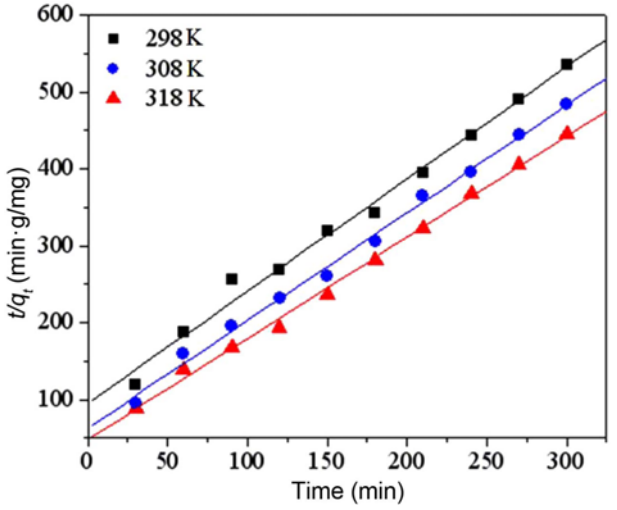

Figure 8. Pseudo-second-order kinetic model for the adsorption of BSA onto TICR.

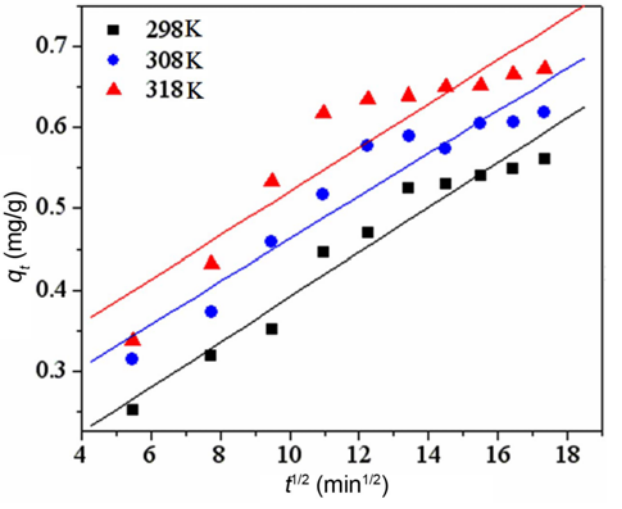

Figure 9. Intrapraticle diffusion model for the adsorption of BSA onto TICR.

equation (4) [37]:

$$\log(q_e - q_t) = \log q_e - \frac{K_1 t}{2.303} \quad (4)$$

where q_e and q_t are the amounts of BSA (mg/g) adsorbed at equilibrium and time t (min), respectively. K_1 is the rate constant of pseudo-first order kinetic model (min^{-1}).

The linear pseudo-second-order equation [38] is referred to as equation (5):

$$\frac{t}{q_t} = \frac{1}{K_2 q_e^{\,2}} + \frac{t}{q_e} \quad (5)$$

where K_2 is the equilibrium rate constant of pseudo-second order equation (g/mg/min), q_t, and q_e are defined as in the pseudo-first order equation.

Figure 8 shows plots of pseudo-second order equation for BSA. The straight lines in plot of linear pseudo-second order equation show good agreement of experimental data with the pseudo-second order kinetic model at 298, 308, and 318 K.

The values of pseudo-first-order equation and pseudo-second order equation parameters together with correlation coefficients are listed in Table 3. The correlation coefficients for the pseudo-first-order equation obtained at all the studied temperatures were low. It suggests that this adsorption process is not a pseudo-first order reaction. The correlation coefficients for the pseudo-second order equation were all over 0.99 at 298, 308, and 318 K. Based on the obtained correlation coefficients, the pseudo-second order equation is the model that furthered the best fit for kinetic data.

The adsorption kinetic data was also analyzed to investigate whether the intraparticle diffusion is the rate-limiting step. The intraparticle diffusion model [39] can be described as equation (6):

$$q_t = K_{id} t^{1/2} \quad (6)$$

where q_t is the amount of BSA adsorbed onto TICR at time t, and K_{id} is the intraparticle diffusion rate constant (mg/g/$min^{1/2}$). If the intraparticle diffusion is the only rate-limiting step, the regression of q_t versus $t^{1/2}$ is linear and passes through the origin [40,41]. The plots are shown in Figure 9. The parameters of intraparticle diffusion model are given in Table 3. As seen from Figure 9, the straight line did not pass through the origin, suggesting that intraparticle diffusion may not be the only rate-limiting step [32].

Evaluation of Adsorption Thermodynamics

To determine the effect of temperature on BSA adsorption, adsorption experiments were also conducted at 298, 308, and 318 K. The thermodynamic parameters such as the changes in Gibbs free energy (ΔG^o), enthalpy (ΔH^o), and entropy (ΔS^o) were determined by using the following

Table 3. Kinetic parameters for BSA adsorption onto TICR

T (K)	Pseudo-first-order equation			Pseudo-second-order equation			Intraparticle diffusion equation	
	K_1 (min^{-1})	q_e (mg/g)	R^2	K_2 (g/mg/min)	q_e (mg/g)	R^2	K_{id} (mg/g/$min^{1/2}$)	R^2
298	0.018	0.473	0.9458	0.022	0.687	0.9901	0.0276	0.9518
308	0.017	0.407	0.9083	0.031	0.714	0.9954	0.0271	0.8531
318	0.010	0.383	0.8576	0.036	0.761	0.9968	0.0264	0.9123

Table 4. Thermodynamic parameters for BSA adsorption onto TICR

T (K)	ΔG^o (J/mol)	ΔS^o (J/mol/K)	ΔH^o (kJ/mol)
298	-223.066		
308	-1016.732	55.457	16.226
318	-1321.623		

equations as equations (7) and (8) [42]:

$$\Delta G^o = -RT \ln q_s \quad (7)$$

$$\ln q_s = \frac{\Delta S^o}{R} - \frac{\Delta H^o}{RT} \quad (8)$$

where R (8.314 J/mol/K)) is the ideal gas constant and T (K) is the temperature. ΔH^o and ΔS^o were calculated from the slope and intercept of plot of ln q_s (from Langmuir isotherm model) versus 1/T. The results of these thermodynamics are displayed in Table 4. The negative values of ΔG^o indicated the spontaneous process of BSA adsorption at 298, 308, and 318 K, and higher negative value reflects a more energetically favorable sorption. The degree of spontaneity of the process also increased in higher temperatures. According to thermodynamics, the ΔH^o value can be used as a measure of the interaction between adsorbate and adsorbent. The positive values of ΔH^o reflected an endothermic adsorption process. The adsorption of BSA is an endothermic process. However, the desorption of water molecules is an endothermic process. When one BSA molecule was adsorbed, more water molecules were desorbed. The positive value of ΔS^0 corresponds to an increase in the degree of freedom of the adsorbed species. The adsorption process was essential for the exchange process of BSA in water solution and adsorbed water molecules on TICR. When BSA was adsorbed onto TICR, much more water molecules might be desorbed from TICR. During the replacement process, due to the molar volume of BSA bigger than the water, the displaced water molecules were more than the adsorbed BSA and the total entropy change in the adsorption process was a positive value. Thus, the adsorption process was likely to occur spontaneously at normal and high temperatures because $\Delta H^o > 0$ and $\Delta S^o > 0$.

Apparent Activation Energy

The apparent activation energy (E_a) can be calculated by using the following Arrhenius expression. An equation is referred to as equation (9) [43]:

$$\ln K = \ln A - \frac{E_a}{RT} \quad (9)$$

where K is the total rate constants and A is a related constant.

The value of E_a of TICR was 1.488 kJ/mol. It indicated that adsorption process for BSA was endothermic. The results showed that increasing temperature is favorable to adsorb BSA with TICR.

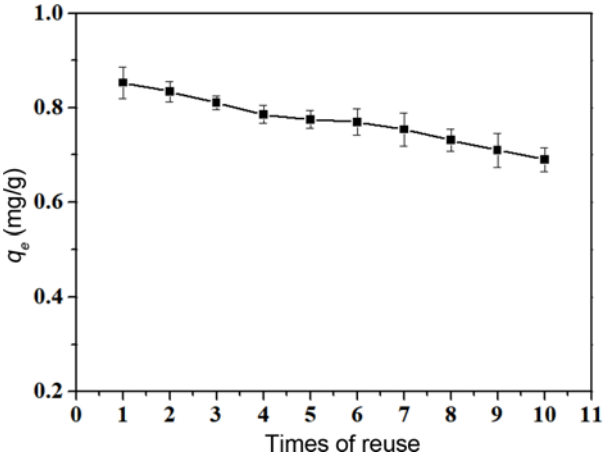

Figure 10. Relationship between the times of reuse and the adsorption capacity of BSA onto TICR.

Desorption and Recycling of TICR

Desorption studies help to reveal the nature of adsorption process and recover BSA from TICR. As can be seen from Figure 10, the adsorption capacity of TICR for BSA decreased slightly from 0.853 to 0.690 mg/g with increasing reuse times. This may be due to that a certain amount of TA molecules were released from TICR during the desorption process. However, TICR could be reused for 10 times with only 19 % loss of adsorption capacity for BSA, which indicated that TICR had a good reusability on the adsorption of BSA.

Conclusion

A novel TA-immobilized chitosan resin (TICR) had shown an efficient adsorption capacity on BSA. The experimental data was well fitted by the Langmuir isotherm model. The kinetic studies indicated that the pseudo-second order describes the adsorption process well. The regression results of the intraparticle diffusion model suggested that intraparticle diffusion was not the only rate-limiting step. The studies of desorption and reusability showed that TICR could be reused for 10 times with about 19 % loss of adsorption capacity for BSA. Therefore, there are good prospects for TICR in practical applications for the removal of protein from aqueous solutions for food industry, such as beer, juice, and aquatic processing wastewater.

References

1. Y. Li, J. Wang, X. Meng, and B. Liu, *J. Food Safety*, **35**, 248 (2015).
2. B. Liu, D. Wang, G. Yu, and X. Meng, *J. Ocean Univ. China*, **12**, 500 (2013).
3. M. J. Boggione, C. R. A. Mahl, M. M. Beppu, and B.

Farruggia, *Powder Technol*., **315**, 250 (2017).
4. C. Hu, P. Zhu, M. Cai, H. Hu, and Q. Fu, *Appl. Clay Sci.,* **143**, 320 (2017).
5. V. Wagener, A. R. Boccaccini, and S. Virtanen, *Appl. Surf. Sci*., **416**, 454 (2017).
6. M. A. Badawi, N. A. Negm, M. T. H. Abou Kana, H. H. Hefni, and M. M. Abdel Moneem, *Int. J. Biol. Macromol.*, **99**, 465 (2017).
7. Y. Luo, Z. Zhou, and T. Yue, *Food Chem*., **221**, 317 (2017).
8. L. Yu, D. Wang, W. Hu, H. Li, and M. Tang, *Front. Chem. China*, **4**, 160 (2009).
9. Y. Wang, X. Wang, G. Luo, and Y. Dai, *Bioresour. Technol*., **99**, 3881 (2008).
10. S. R. Popuri, Y. Vijaya, V. M. Boddu, and K. Abburi, *Bioresour. Technol*., **100**, 194 (2009).
11. G. R. Mahdavinia, A. Pourjavadi, H. Hosseinzadeh, and M. J. Zohuriaan, *Eur. Polym. J.*, **40**, 1399 (2004).
12. C. Hu, Y. Deng, H. Hu, Y. Duan, and K. Zhai, *Int. J. Biol. Macromol*., **92**, 1191 (2016).
13. J. Ananpattarachai and P. Kajitvichyanukul, *J. Cleaner Prod.*, **130**, 126 (2016).
14. W. Hua, Y. Lou, W. Xu, Z. Cheng, X. Gong, and J. Huang, *Appl. Microbiol. Biotechnol*., **100**, 879 (2016).
15. R. Zeng, Y. Zhang, Z. H. Liang, M. Tu, and C. R. Zhou, *Sci. China Ser. E: Technol. Sci*., **52**, 2275 (2009).
16. S. Rivero, M. A. Garca, and A. Pinotti, *Carbohydr. Polym.*, **82**, 270 (2010).
17. B. Kaczmarek, A. Sionkowska, and A. M. Osyczka, *Polym. Test*., **65**, 163 (2018).
18. M. Yurtsever and I. A. Şengl, *Trans. Nonferrous Met. Soc. China*, **22**, 2846 (2012).
19. C. Yu, J. Geng, Y. Zhuang, J. Zhao, L. Chu, X. Luo, Y. Zhao, and Y. Guo, *Carbohydr. Polym.*, **152**, 327 (2016).
20. X. Huang, X. Liao, and B. Shi, *J. Hazard. Mater.*, **170**, 1141 (2009).
21. X. Sun, X. Huang, X. Liao, and B. Shi, *J. Hazard. Mater.*, **179**, 295 (2010).
22. A. M. Omer, T. M. Tamer, M. A. Hassan, P. Rychter, M. S. Mohy Eldin, and N. Koseva, *Int. J. Biol. Macromol*., **92**, 362 (2016).
23. Z. Wang, T. Yue, Y. Yuan, R. Cai, C. Niu, and C. Guo, *Int. J. Biol. Macromol*., **58**, 57 (2013).
24. J. M. N. dos Santos, C. R. Pereira, E. L. Foletto, and G. L. Dotto, *Int. J. Biol. Macromol*., **131**, 301 (2019).
25. J. Du, Y. Q. Zhou, L. L. Wang, and Y. C. Wang, *Carbohydr. Polym.*, **153**, 471 (2016).
26. B. J. Liu, D. F. Wang, X. Gao, L. Zhang, Y. Xu, and Y. J. Li, *Eur. Food Res. Technol.*, **232**, 911 (2011).
27. S. S. T. Gülmen, E. A. Güvel, and N. Kızılcan, *Procedia Soc. Behav. Sci.*, **195**, 1623 (2015).
28. H. Zhu, R. Jiang, L. Xiao, and G. Zeng, *Bioresour. Technol*., **101**, 5063 (2010).
29. Q. Shi, Y. Tian, X. Dong, S. Bai, and Y. Sun, *Biochem. Eng. J*., **16**, 317 (2003).
30. M. Monier and D. A. Abdel-Latif, *J. Hazard. Mater.*, **209-210**, 240 (2012).
31. F. G. L. Medeiros Borsagli, A. A. P. Mansur, P. Chagas, L. C. A. Oliveira, and H. S. Mansur, *React. Funct. Polym.*, **97**, 37 (2015).
32. S. H. Chang and C. H. Chian, *Appl. Surf. Sci.*, **282**, 735 (2013).
33. Z. C.Wu, Z. Z.Wang, J. Liu, J. H. Yin, and S. P. Kuang, *Int. J. Biol. Macromol*., **81**, 838 (2015).
34. J. Qi, P. Yao, F. He, C. Yu, and C. Huang, *Int. J. Pharm.*, **393**, 177 (2010).
35. C. Cao, L. Xiao, C. Chen, X. Shi, Q. Cao, and L. Gao, *Powder Technol*., **260**, 90 (2014).
36. W. S. Wan Ngah, M. A. K. M. Hanafiah, and S. S. Yong, *Colloids Surf*., *B*, **65**, 18 (2008).
37. M. Ghaemy and M. Naseri, *Carbohydr. Polym.*, **90**, 1265 (2012).
38. X. Liu and L. Zhang, *Powder Technol*., **277**, 112 (2015).
39. Y. Wang, X. Wang, G. Luo, and Y. Dai, *Bioresour. Technol*., **99**, 3881 (2008).
40. H. Ding, J. Q. Li, Y. J. Gao, D. Zhao, D. J. Shi, G. Z. Mao, S. J. Liu, and X. Tan, *Powder Technol*., **284**, 231 (2015).
41. V. Nair, A. Panigrahy, and R. Vinu, *Chem. Eng. J.*, **254**, 491 (2014).
42. A. L. Ahmad, C. Y. Chan, S. R. Abd Shukor, and M. D. Mashitah, *Chem. Eng. J.*, **148**, 378 (2009).
43. I. Lakhdhar, P. Mangin, and B. Chabot, *J. Water Process Eng*., **7**, 295 (2015).